Insights Imaging (2012) 3:277–293
DOI 10.1007/s13244-012-0155-2

PICTORIAL REVIEW

Fetal MR in the evaluation of pulmonary and digestive system pathology

César Martin · Anna Darnell · Conxita Escofet · Carmina Duran · Víctor Pérez

Received: 6 November 2011 / Revised: 2 February 2012 / Accepted: 20 February 2012 / Published online: 18 April 2012
© European Society of Radiology 2012

Abstract
Background Prenatal awareness of an anomaly ensures better management of the pregnant patient, enables medical teams and parents to prepare for the delivery, and is very useful for making decisions about postnatal treatment. Congenital malformations of the thorax, abdomen, and gastrointestinal tract are common. As various organs can be affected, accurate location and morphological characterization are important for accurate diagnosis.
Methods Magnetic resonance imaging (MRI) enables excellent discrimination among tissues, making it a useful adjunct to ultrasonography (US) in the study of fetal morphology and pathology.
Results MRI is most useful when US has detected or suspected anomalies, and more anomalies are detected when MRI and US findings are assessed together.
Conclusion We describe the normal appearance of fetal thoracic, abdominal, and gastrointestinal structures on MRI, and we discuss the most common anomalies involving these structures and the role of MRI in their study.
Teaching Points
- *To learn about the normal anatomy of the fetal chest, abdomen, and GI tract on MRI.*
- *To recognize the MR appearance of congenital anomalies of the lungs and the digestive system.*
- *To understand the value of MRI when compared to US in assessing fetal anomalies.*

Keywords Congenital abnormalities · Imaging, magnetic resonance imaging · Thorax · Gastrointestinal tract · Abdomen

C. Martin · A. Darnell · C. Escofet · C. Duran · V. Pérez
Radiology Department, UDIAT CD,
Institut Universitari Parc Taulí-UAB,
Sabadell, Spain

A. Darnell (✉)
Radiology Department, Hospital Clínic,
Barcelona, Spain
e-mail: andarnel@clinic.ub.es

Introduction

Prenatal diagnosis aims to obtain genetic, anatomic, biochemical, and physiological information about the fetus to detect fetal anomalies that can have an influence during the gestational period or after birth. Some anomalies may be asymptomatic after birth, and prenatal detection enables early diagnosis and rapid intervention to minimize complications. Parents need accurate information, genetic counseling, and therapeutic options for any anomaly detected prenatally.

Ultrasonography (US) is the imaging method of choice for screening and evaluating fetal anomalies, and magnetic resonance imaging (MRI) provides excellent discrimination among tissues, making it a useful complementary noninvasive technique in the study of fetal morphology and pathology. Congenital malformations of the thorax, abdomen, and gastrointestinal tract are common. As various organs can be affected, accurate location and morphological characterization are important for diagnosis.

We describe the normal appearance of fetal thoracic, abdominal, and gastrointestinal structures on MRI, discuss the most common anomalies involving these structures, and define the role of MR in their study.

We do not discuss urogenital tract anomalies in this article.

MRI technique

In our institution MRI is done after US, during the same gestational week whenever possible. Radiologists are always aware of suspected US anomalies. Pathologic findings are confirmed with postnatal imaging, autopsy, surgical pathologic examination, or clinical follow-up.

Before MRI, both parents are informed about the imaging procedure and possible implications of imaging findings.

Patients are asked to urinate before the procedure to avoid the urge to urinate. They are normally placed in the supine position and introduced feet-first to minimize claustrophobia. No medication is administered to prevent fetal movements.

We routinely use the half-Fourier single-shot turbo spin-echo (HASTE) sequence. Occasionally, thick-slab highly T2-weighted or T1-weighted sequences are used. For the volumetric, highly T2-weighted sequences, we use the single-shot rapid acquisition with relaxation enhancement sequence. One 50- to 100-mm-thick slab is obtained in 4 to 7 s. For the T1-weighted sequences, the fast low-angle shot (FLASH) sequence with maternal breath-hold is used. Our study protocol includes a scouting acquisition, followed by a series of HASTE sequences in the axial, coronal, and sagittal planes of the maternal abdomen to evaluate maternal abdominal organs, uterine anatomy, the placenta, the amount of amniotic fluid, and fetal position. Next, a series of coronal, axial, and sagittal sequences of the different regions of the fetus are obtained. The thorax and abdomen of the fetus are in the same plane and can be studied together. The brain is usually in a different plane from the thorax and abdomen, and therefore usually needs to be studied independently. We normally position each sequence over the immediately prior one to avoid oblique planes due to fetal motion [1, 2].

Normal anatomy of the fetal thorax, gastrointestinal tract, and abdomen

T2-weighted single-shot fast spin-echo images show the major thoracic, abdominal, and gastrointestinal tract structures clearly. T1-weighted sequences are especially useful in the evaluation of the digestive tract; in these sequences the stomach and small intestine are hypointense, whereas the large intestine is hyperintense due to its contents (meconium) [3].

Thorax

The diaphragm separating the chest from the abdomen is visible in coronal and sagittal images. Normal fetal lungs are hyperintense, because they typically contain a significant amount of alveolar fluid, and the trachea and bronchi are normally seen as hyperintense tubular structures. The normal thymus is well visualized on MRI, especially in the third trimester. It is easily identified in HASTE sequences as a structure with homogeneous signal intensity that is lower than that of the lungs but higher than that of the heart in the anterior mediastinum, usually above the heart. The size of the thymus varies, and it can be quite large in the third trimester.

Heart defects can be evaluated better with US than with MRI; however, MRI can be useful for evaluating some heart conditions like anomalous position, cardiomegaly, pericardial effusion, and even tumors within the heart like rhabdomyoma.

Gastrointestinal tract

The esophagus is rarely seen on MRI unless it is pathologically dilated or image acquisition coincides with fetal swallowing. When it is seen, the esophagus is seen on T2-weighted images as a hyperintense tubular structure behind the trachea. In T2-weighted sequences, the stomach should be seen, even early in gestation, as a hyperintense cavity, and the jejunum and ileum are identified as hyperintense serpiginous structures distributed throughout the abdomen but mainly occupying the left hemiabdomen. The large intestine is hypointense at T2 and hyperintense at T1, owing to the presence of meconium. These structures should be evaluated in the axial, coronal, and sagittal planes of the fetal abdomen. The rectal ampulla is best evaluated on T1-weighted images in the midline sagittal plane.

Liver, spleen, pancreas, peritoneal cavity, and abdominal wall

The liver is well depicted in all planes. It is fairly hypointense on T2-weighted sequences and has intermediate signal intensity on T1-weighted images. The gallbladder is well visualized and is hyperintense on T2-weighted sequences. The spleen is more difficult to see; its signal intensity is somewhat greater than that of the liver at T2. The pancreas is not usually seen, possibly due to its small size. The peritoneal cavity is a virtual cavity that is not usually seen except when ascites is present. The abdominal wall is easily identified in T2-weighted sequences in all planes. The umbilical cord and its place of insertion are also easily recognizable, especially in the midline sagittal and axial planes. Volumetric sequences can be very helpful in the evaluation of the umbilical cord (Figs. 1 and 2).

Thoracic anomalies

Congenital diaphragmatic hernia

Congenital diaphragmatic hernias are rare; most are left sided, and less than 5% are bilateral [4]. They are caused

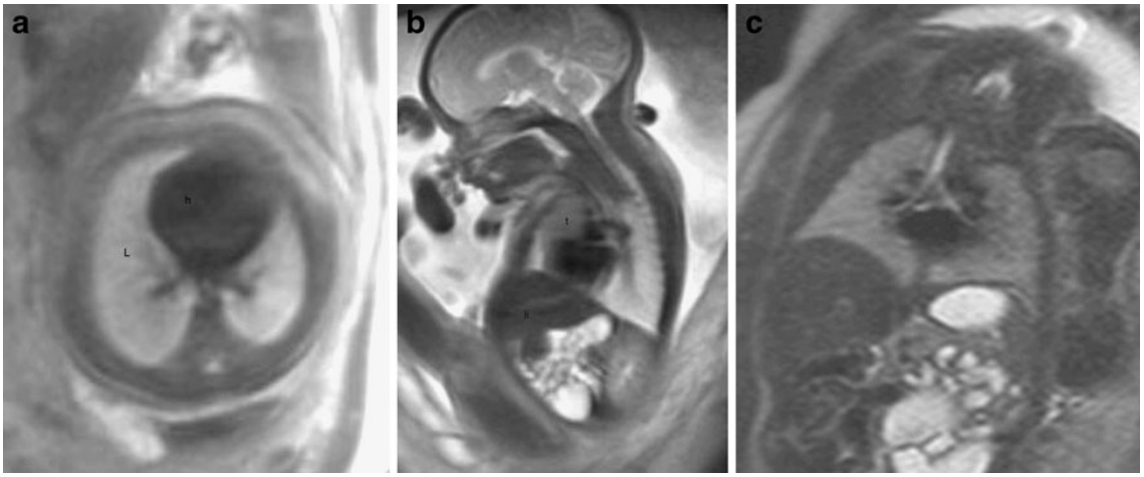

Fig. 1 Normal fetal anatomy of the thoracoabdominal region. Fetus at 28 weeks' gestation. **a**, **b** and **c** Fetal axial, sagittal, and coronal single-shot fast spin-echo MR images showing some normal fetal structures: *h* heart, *L* lungs, *t* thymus, and *li* liver. The trachea and bronchi are seen as hyperintense tubular structures in (**c**)

by a defect in the diaphragmatic musculature. In left-sided hernias, the stomach is often herniated but sometimes it is in its normal position; occasionally, part of the liver is also herniated. In right-sided hernias herniation of the liver is nearly always present. Herniation of abdominal structures into the chest leads to different degrees of pulmonary hypoplasia and pulmonary hypertension, and the prognosis depends on these conditions.

MRI's excellent tissue contrast resolution allows easy differentiation between organs. Thus, structures like small bowel loops and lungs that can have similar appearances on US are clearly differentiated on MRI, enabling herniated abdominal structures to be identified (Figs. 3 and 4).

MRI is also useful in the evaluation of fetal lung maturation through volume [5, 6]. Moreover, the amount of fluid in the lungs increases throughout gestation; thus, lung signal intensity also increases, and this can provide us with an indirect sign of lung maturation. If the signal intensity and volume of the lungs are appropriate, the prognosis is often good. Some groups are using MRI to evaluate lung changes after fetoscopic endoluminal tracheal occlusion [7].

Eventration of the diaphragm is usually impossible to distinguish from diaphragmatic hernia on MRI; nevertheless, the repercussions during the pregnancy and later medical management are normally the same.

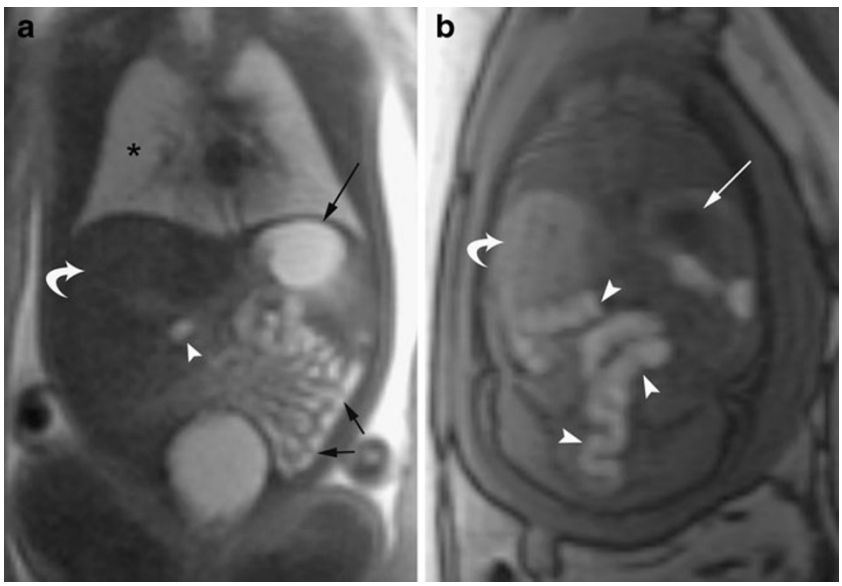

Fig. 2 Normal fetal anatomy of the thoracoabdominal region. Fetus at 26 weeks' gestation. **a** Fetal coronal single-shot fast spin-echo MR image showing many fetal structures: lungs (*asterisk*), stomach (*long arrow*), small intestine (*short arrows*), liver (*curved arrow*), and gallbladder (*arrowhead*). **b** Coronal T1-weighted gradient-echo FLASH sequence showing the stomach (*long arrow*), large intestine (*arrowheads*), and liver (*curved arrow*)

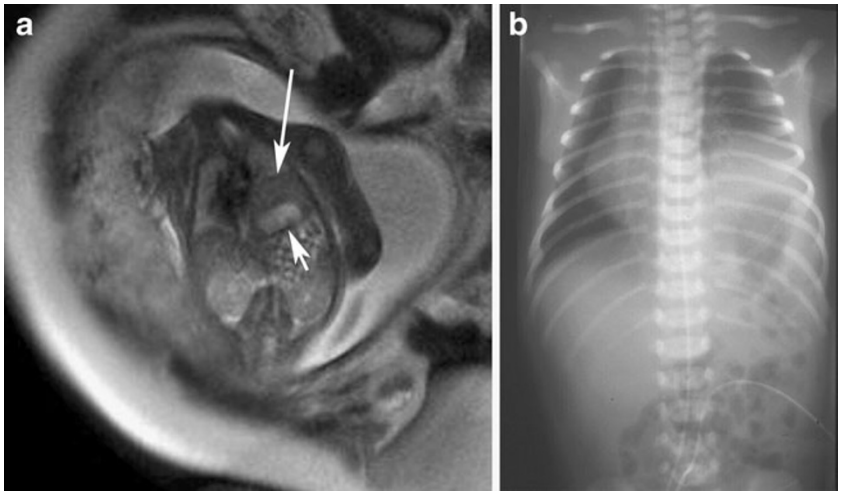

Fig. 3 Left congenital diaphragmatic hernia. Fetus at 27 weeks' gestation. **a** Coronal image of the fetal chest and abdomen. Elevation of the left diaphragm (*long arrow*); we can see the fetal stomach full of fluid (*short arrow*). **b** X-ray after birth shows the same findings

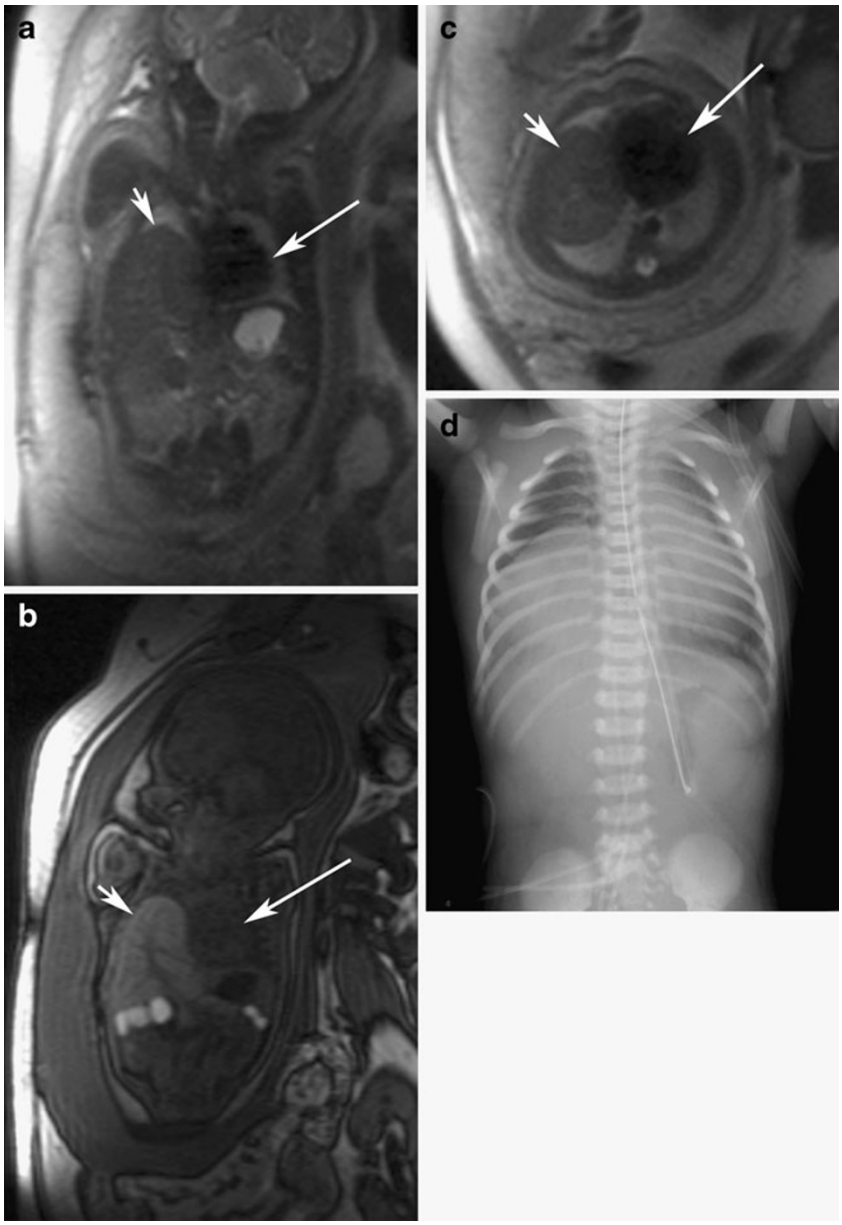

Fig. 4 Right congenital diaphragmatic hernia. Fetus at 36 weeks' gestation. **a** Fetal coronal single-shot fast spin-echo MR image and **b** T1-weighted fetal coronal image show the diaphragmatic hernia. Part of the liver (*short arrow*) is in the chest and the heart (*long arrow*) is displaced slightly to the left. **c** Fetal axial single-shot fast spin-echo MR image shows part of the liver (*short arrow*) in the chest and the leftward shift of the heart (*long arrow*). **d** X-ray after birth

Congenital cystic adenomatoid malformation (CCAM)

CCAM is the most commonly diagnosed lung malformation. The real incidence of this anomaly is unknown because most cases are asymptomatic and CCAM sometimes regresses during the second half of pregnancy.

In CCAM, abnormal branching of the immature bronchioles and lack of normal alveolar development results in a solid/cystic intrapulmonary mass. Three types have been described depending on the presence of macro- or microcysts; depending on the type they are seen on MRI as cystic or solid hyperintense lesions in the thorax (Fig. 5). The prognosis depends on the degree of pulmonary hypoplasia associated with the size of the mass.

The differential diagnosis should be made with bronchopulmonary sequestration, and this distinction is difficult before birth, especially in the case of mixed lesions.

CCAMs usually become smaller as the pregnancy advances and may go undetected at postnatal clinical examination and chest X-rays, so a CT is necessary to confirm their presence and to plan treatment. CCAMs are usually excised because of their increased risk of infection and malignant potential [8, 9].

Bronchopulmonary sequestration

Pulmonary sequestration is a supernumerary lung lobe that results from a foregut malformation. Most sequestrations detected prenatally are extralobar, with an anomalous vein that drains into the systemic circulation. Most are left-sided, and up to 10% are infradiaphragmatic, making it necessary to differentiate them from neuroblastomas; however, unlike neuroblastomas, sequestrations can appear in the second trimester [8, 10].

On T2-weighted images they are seen as well-defined hyperintense masses with or without hypointense septa [11] (Figs. 6 and 7). Intralobar sequestration may be difficult to differentiate from CCAM, because the systemic feeding vessel is often difficult to detect.

Fig. 5 Congenital cystic adenomatoid malformation. Fetus at 22 weeks' gestation. **a**, **b** and **c** Fetal sagittal, coronal, and axial single-shot fast spin-echo MR images of the fetal chest show a complex hyperintense lesion with cysts inside in the right lung (*arrows*). CT after birth **d** shows the lesion, which is proportionally smaller than in the MR images

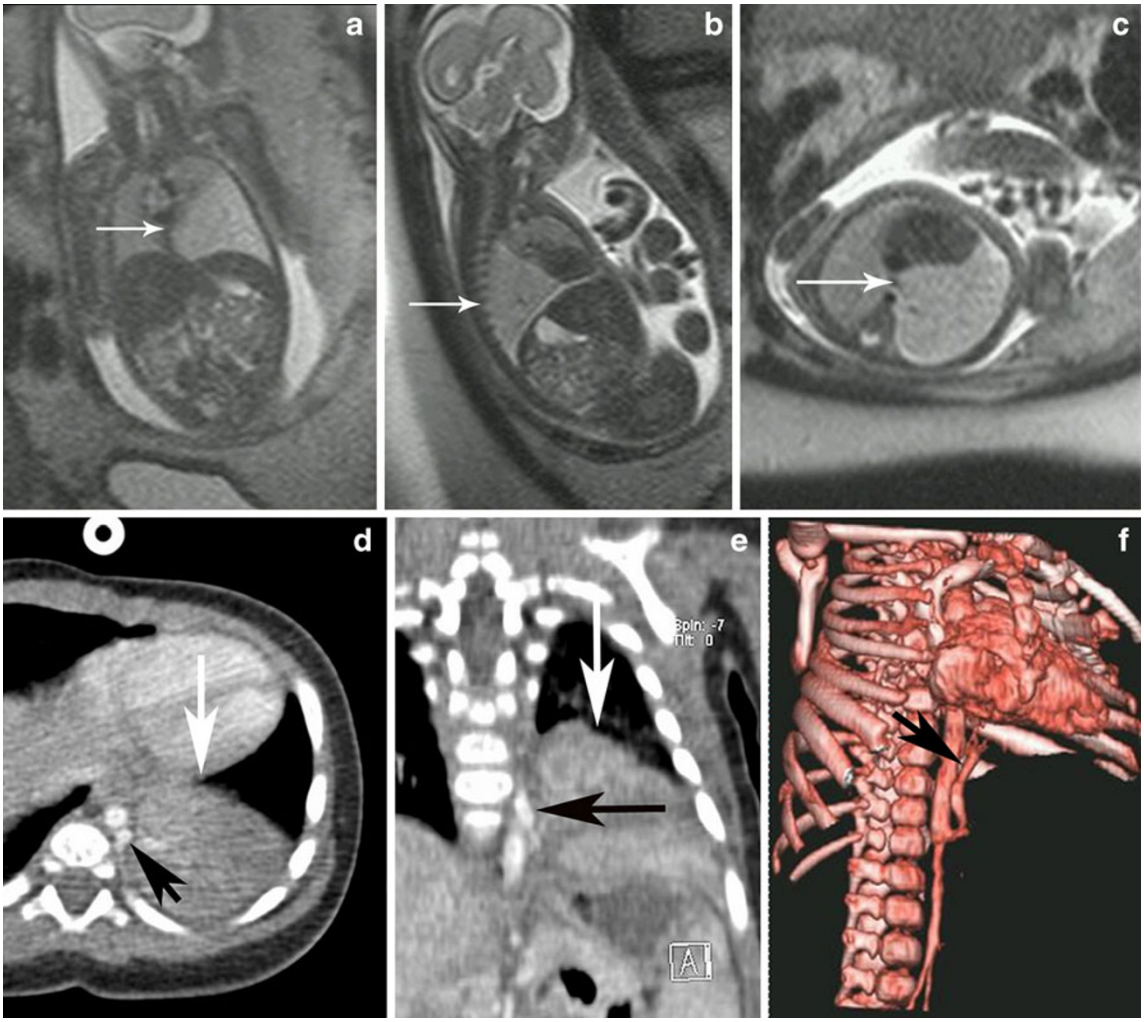

Fig. 6 Extralobar bronchopulmonary sequestration. Fetus at 23 weeks' gestation. **a**, **b** and **c** Fetal coronal, sagittal, and axial single-shot fast spin-echo MR images of the fetal chest show a hyperintense anomalous area in the left lung (*arrows*). **d**, **c** and **f** CT after birth shows bronchopulmonary sequestration (*white arrows*) and the systemic vessel (*black arrows*) that feeds the lesion

Bronchopulmonary sequestrations sometimes shrink during pregnancy, and the prognosis is usually good. Postnatal CT normally shows the anomalous vessels that are difficult to detect prenatally.

MRI is also useful for evaluating other pulmonary and thoracic anomalies. Bronchogenic cysts are identified as hyperintense lesions in HASTE sequences; they are usually single lesions, located in the lung or mediastinum. Esophageal duplication cysts are also identified as hyperintense mediastinal lesions. Congenital lobar emphysema can be difficult to distinguish from intralobar sequestration and from CCAM, because MRI shows all these lesions as space-occupying lesions with increased signal intensity on HASTE sequences. Congenital mediastinal masses like teratomas and cystic lymphangiomas are easily diagnosed on MRI.

Gastrointestinal tract anomalies

Proximal gastrointestinal tract disorders

Esophageal atresia

Incomplete division of the foregut into the ventral respiratory portion and the dorsal digestive portion by the tracheoesophageal septum results in esophageal atresia. The most common condition is atresia with distal tracheoesophageal fistula (90% of cases) [12].

MRI findings are polyhydramnios and absent or very small stomach. However, a small stomach may be a normal finding or may have other causes (deglution disorders, facial defects, cervicofacial tumors, CNS lesions, oligohydramnios, etc.). Occasionally the proximal segment of the esophagus can be

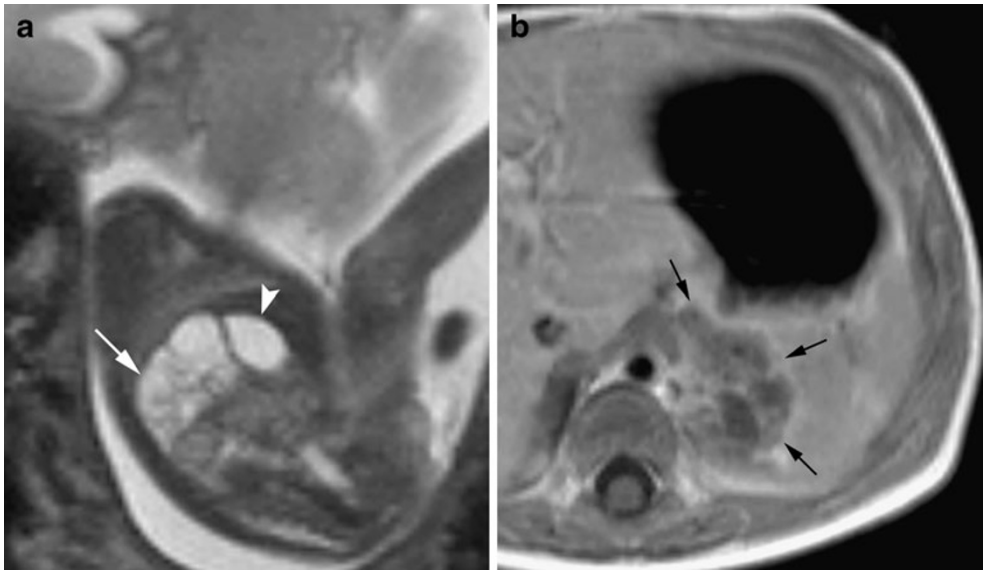

Fig. 7 Infradiaphragmatic extralobar pulmonary sequestration. Fetus at 23 weeks' gestation. **a** Fetal sagittal single-shot fast spin-echo MR image showing a well-defined hyperintense mass with hypointense septa in the left abdomen (*arrow*) between the diaphragm, the stomach (*arrowhead*), and above the kidney. Imaging studies after birth (US, CT, and MR) detected this lesion; the suprarenal gland was normal and the metaiodobenzylguandine study was negative. **b** Postnatal axial T1-weighted MR image showing the lesion (*arrows*). The child is asymptomatic, and the laboratory tests were normal. No anomalous vascular irrigation was detected; nevertheless, we believe this is a case of infradiaphragmatic extralobar pulmonary sequestration, and no surgery has been performed

seen as a hyperintense pouch in T2-weighted sequences, especially in sagittal images along the midline of the fetal thorax [13, 14] (Fig. 8). Tracheoesophageal fistulas are not normally seen on MRI.

Associated anomalies are present in 50% to 70% of cases, and esophageal atresia is sometimes associated with chromosomopathies, especially Down's syndrome [12].

Duodenal obstruction

Duodenal obstruction can be caused by atresia or stenosis, which might be caused by vascular impairment during gut development, intraluminar diaphragm, annular pancreas, intestinal malrotation with Ladd's band, or volvulus of the middle portion of the intestine. Duodenal atresia and annular pancreas are often associated [15].

In cases of duodenal atresia or marked duodenal obstruction, MRI shows dilatation of the stomach and the portion of the duodenum proximal to the obstruction as hyperintense structures in T2-weighted sequences (Fig. 9). When obstruction is due to malrotation with Ladd's band or volvulus, the loops of the small intestine can be seen lying mostly on the right side of the abdomen while the colon is on the left (Fig. 9); the colon is best visualized on T1-weighted sequences. The stomach and duodenum may be normal sized or even small when the fetus also has esophageal atresia. Polyhydramnios is almost always present.

Approximately 50% of cases of duodenal obstruction have associated gastrointestinal, genitourinary, cardiac, skeletal, or chromosomal anomalies; trisomy 21 is often associated [15–17].

Small bowel abnormalities (jejunum and ileum)

At approximately 20 weeks' gestation, the US appearance of the large and small intestines is very similar to the rest of abdominal structures (liver, spleen, kidneys); furthermore, US cannot differentiate between the large and small intestines. The MRI behavior of intestinal contents is well established [3]. In T2-weighted sequences, the signal intensity of intestinal contents decreases as they descend through the gastrointestinal tract, so that the stomach and small bowel loops are hyperintense and the colon is hypointense. Inverse findings are seen on T1-weighted sequences, i.e., the signal intensity of intestinal contents increases as they descend through the gastrointestinal tract. Thus, both the small and large intestines are well depicted early in gestation, and MRI can detect and characterize intestinal anomalies with greater accuracy than US in this period.

Atresia

Atresia is probably caused by vascular impairment during gut development [18]. Atresia is most common in the distal ileum, followed by the proximal jejunum; multiple atresia is not uncommon.

MRI detects dilatation of the small intestine proximal to the atresia; the stomach and duodenum may also be dilated.

Fig. 8 Esophageal atresia with distal tracheoesophageal fistula. Fetus at 33 weeks' gestation. MR was indicated for US findings of renal ectopia or horseshoe kidney. **a** and **b** Sagittal single-shot fast spin-echo MR images of the fetus. MR detected left renal agenesis and ectopia of the right kidney (*arrow* in **a**). A pouch was detected in the upper esophagus (*arrow* in **b**). There was polyhydramnios, and the stomach was small. **c** and **d** CT after birth showing the atresia and the tracheoesophageal fistula (*arrow* in **d**), *T* trachea, *E* esophagus

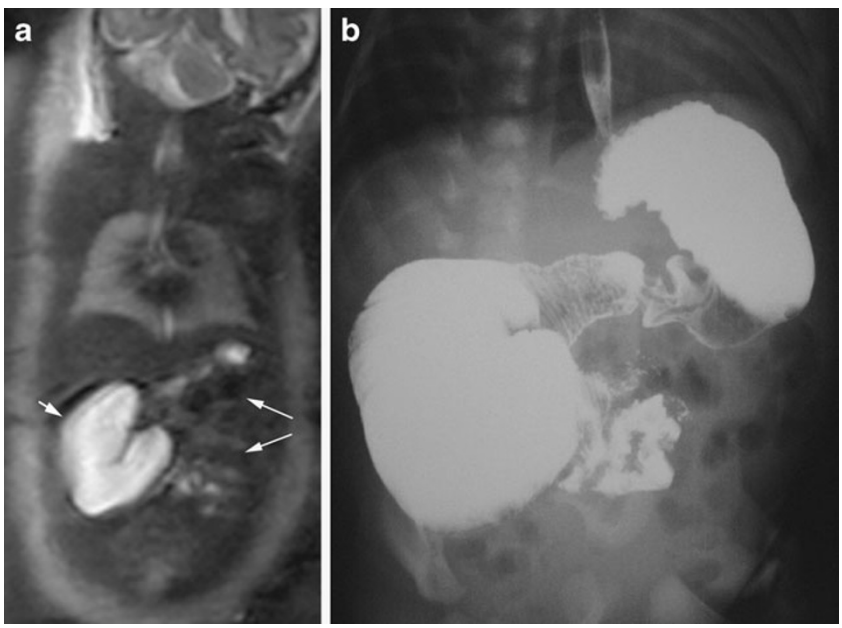

Fig. 9 Duodenal stenosis due to Ladd's band. Fetus at 32 weeks' gestation. **a** Fetal coronal single-shot fast spin-echo MR image: the duodenum is greatly dilated until the third portion (*short arrow*); the stomach seems normal; there may be gastroesophageal reflux. The volume of amniotic fluid is normal. The large bowel is in the left abdomen (*long arrows*). **b** X-rays after birth showing marked dilatation of the duodenum. At surgery, intestinal malrotation and Ladd's band causing duodenal occlusion were found, as well as Meckel's diverticulum, which was undetected at US and MR

The signal intensity of the contents of the intestine varies in relation to the site of obstruction; the more distal the obstruction is, the lower the signal intensity on T2-weighted images and the higher the signal intensity on T1-weighted images [3] (Fig. 10). The colon may be small in caliber or impossible to identify. The more proximal the lesion is, the more likely the fetus will have polyhydramnios.

Extraintestinal anomalies are less frequently associated than in duodenal atresia, and the most common associations are with other intestinal anomalies that might be related to the cause of the atresia and to atresias in other locations [15, 19]. A higher incidence of cystic fibrosis has been reported in children with intestinal atresia [20].

Small bowel atresia can be very difficult to differentiate from meconium ileus, volvulus, or Hirschsprung's disease.

Meconium ileus

This condition is caused by functional obstruction of the distal ileum by very dense meconium. It is the earliest manifestation of cystic fibrosis. Nearly all newborns with meconium ileus have cystic fibrosis, and 10% to 15% of all patients with cystic fibrosis have meconium ileus [21].

The MRI findings include dilatation of small bowel loops secondary to meconium impaction, microcolon, and polyhydramnios. Ascites may be present when the condition is complicated by intestinal perforation.

Meconium ileus is often associated to gastrointestinal anomalies like volvulus, jejunoileal atresia, intestinal perforation, and meconium peritonitis.

The differential diagnosis should include jejunoileal atresia, volvulus, and Hirschsprung's disease.

Meconium peritonitis

This condition results from intestinal perforation during fetal life. The release of meconium and digestive enzymes into the peritoneal cavity causes chemical peritonitis resulting in an inflammatory reaction and the formation of fibrous tissue that may calcify. Sometimes the inflammatory response seals the perforation spontaneously.

In most cases, meconium peritonitis is associated to meconium ileus, intestinal atresia, or intestinal volvulus. Intestinal ischemia due to occlusion or mesenteric thrombosis, which may be idiopathic or secondary to intrauterine infection, can also cause intestinal perforation and consequent meconium peritonitis. As meconium ileus is a frequent cause of meconium peritonitis, cystic fibrosis is common in these fetuses.

Ascites and dilatation of the small intestine can be detected with MRI. This is best done using T2-weighted sequences (Fig. 11). Peritoneal calcifications are difficult to appreciate on MRI, as they tend to be small and linear. When seen, they are hypointense in both T1- and T2-weighted sequences. A meconium pseudocyst may result from a contained perforation [22]. Polyhydramnios may also be present.

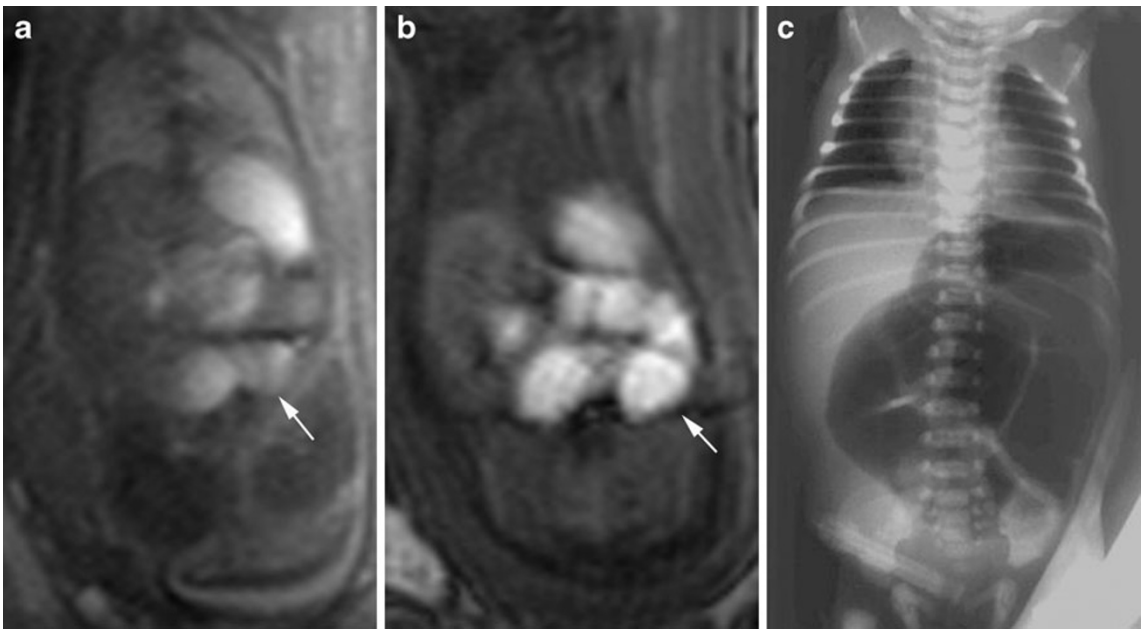

Fig. 10 Jejunal atresia. Fetus at 25 weeks' gestation. **a** Fetal coronal single-shot fast spin-echo MR image and **b** fetal coronal T1-weighted gradient-echo flash image showing dilatation of the proximal portion of the small intestine (*arrows*). **c** X-ray after birth showing dilatation of the proximal intestinal loops. Opaque enema X-ray study showed microcolon, and jejunal atresia was discovered at surgery

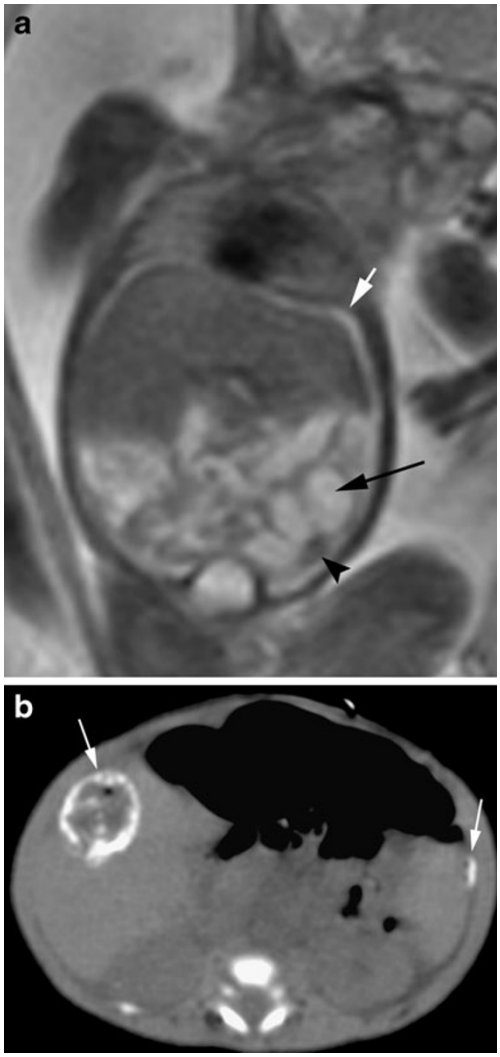

Fig. 11 Meconium peritonitis. Fetus at 26 weeks' gestation. **a** Fetal coronal single-shot fast spin-echo MR image showing a small amount of ascites (*short arrow*) and dilatation of intestinal loops (*long arrow*); a small hypointense area is seen in the left hemiabdomen (*arrowhead*), suggestive of peritoneal calcification. **b** CT after birth shows peritoneal calcifications and a meconium pseudocyst (*arrows*)

Large bowel

Atresia of the colon, anorectal atresia, and cloacal malformations

Fetal MRI allows assessment of the rectum and its contents, and can also provide additional information that can be useful for the diagnosis of anal atresia and other anomalies in the spectrum of cloacal malformations.

Atresia of the colon and anorectal atresia are uncommon and, as in other atresias, vascular impairment seems the most likely etiology. Intestinal loops above the atresia may be dilated, and meconium accumulated above the atresia may cause high signal intensity on T1-weighted sequences (Fig. 12) [22]. The differential diagnosis should include other causes of intestinal dilatation, atresia of the colon, and Hirschsprung's disease.

Cloacal malformations represent a spectrum of developmental defects that usually affect female fetuses. In these malformations, the urinary tract, the vagina, and the rectum converge above the level of the perineum, creating a common channel with a single external opening. It should be suspected in cases of dilation and high position of the distal bowel and abnormalities in the genitourinary system [23].

Other bowel anomalies

Heterotaxy syndromes

The heterotaxy syndromes are a group of rare anomalies characterized by an abnormal arrangement of thoracic and abdominal organs. Abdominal anomalies are very common in this syndrome (multiple spleens, absent spleen, central or left-sided liver, small stomach, central or right-sided stomach, esophageal atresia, duodenal atresia, biliary atresia, intestinal malrotation); heart defects and abnormal bronchial morphology are also common [24].

MRI findings depend on the type of anomaly and on associated anomalies. The easiest to detect is the size and position of the stomach; the position of the liver and heart are also easy to determine, although possible associated heart defects cannot usually be evaluated by MRI. Depending on gestational age, thoracic and abdominal systemic vessel anomalies can also be detected [13]. Asplenia and polysplenia can be difficult to evaluate with MRI (Figs. 13 and 14).

Abdominal anomalies

Abdominal masses

Enteric duplication cyst

Duplications of the digestive tube are uncommon congenital abnormalities found anywhere along the alimentary tract from the tongue to the anus. Intestinal duplication takes place on the mesenteric side of the intestine and does not usually communicate with the intestinal lumen. The most common site of duplication is the distal portion of the ileum, followed by the distal portion of the esophagus and stomach.

Duplication cysts rarely cause intrauterine intestinal occlusion; however, they may cause intestinal occlusion or abdominal pain after birth, due to volvulus, invagination, or bleeding of the cyst.

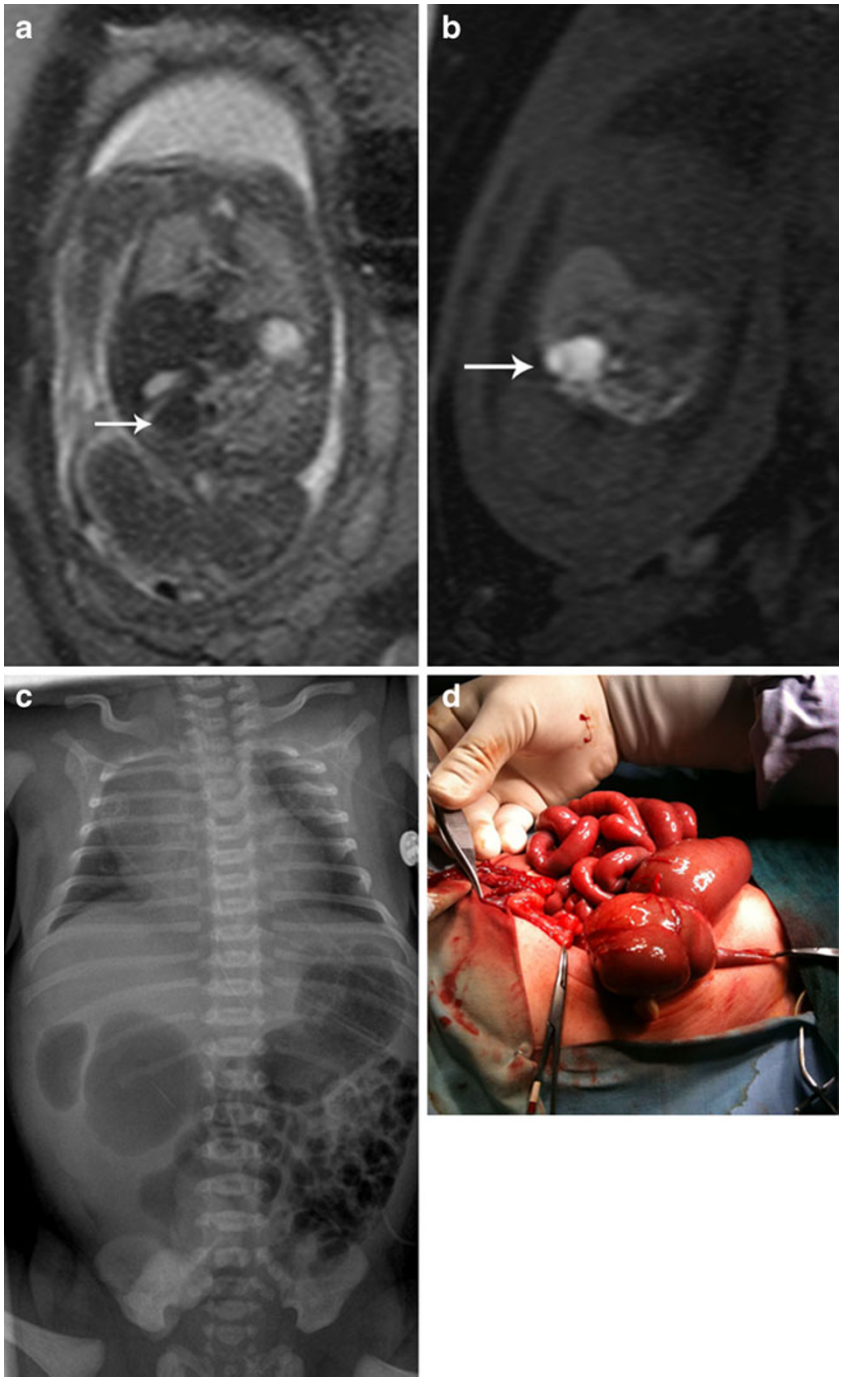

Fig. 12 Cecal atresia. Fetus at 22 weeks' gestation. **a** Fetal coronal single-shot fast spin-echo MR image and **b** fetal coronal T1-weighted gradient-echo flash image. In the right hemiabdomen, below the liver there is a dilated bowel loop hypointense on T2- and hyperintense on T1-weighted images (*arrows*), due to meconium. **c** Abdominal X-ray after birth shows a dilated bowel loop. **d** At surgery cecal atresia was found

On MRI, they are seen as rounded intraabdominal cystic masses adjacent to the bowel. They are hyperintense on T2-weighted sequences and hypointense on T1-weighted sequences [22, 25] (Fig. 15). The rest of the intestinal loops tend to be normal in shape, and polyhydramnios is not usually associated.

T1-weighted sequences can be useful for differentiating these anomalies from dilated intestinal loops. They can be difficult to differentiate prenatally from other abdominal cysts like mesenteric cyst, choledochal cyst, and specially ovarian cysts. Ovarian cysts are common during the prenatal period; they are usually detected in the third trimester of pregnancy [26]. Most are unilateral although they can be bilateral. Overstimulation of the ovaries by placental and maternal hormones seems to play an important role in their formation. In the fetal period, they may be simple cysts or they can become complicated with torsion and bleeding. On MRI, simple cysts are seen as an intraabdominal cystic

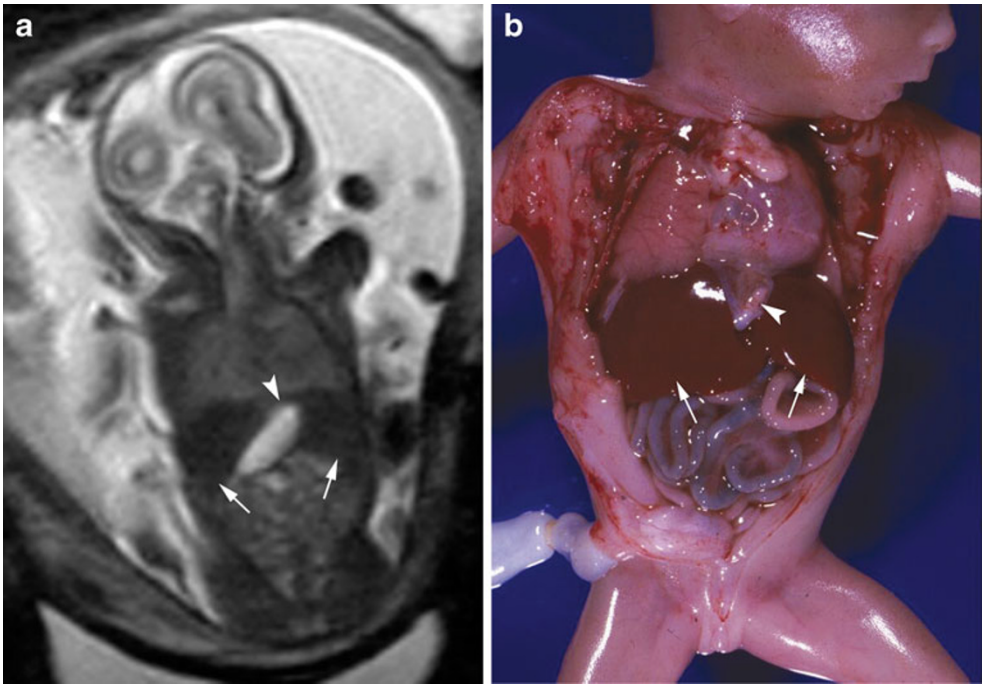

Fig. 13 Heterotaxy syndrome, polysplenia syndrome. Fetus at 20 weeks' gestation. **a** Fetal coronal single-shot fast spin-echo MR image in which the liver (*arrows*) and stomach (*arrowhead*) are centrally located; the multiple spleens present were not seen at MR. **b** Anatomical specimen showing these anomalies: liver (*arrows*), stomach (*arrowhead*). This fetus had heart defects

structure that is hyperintense on T2-weighted sequences and hypointense on T1-weighted sequences. When complicated by torsion and/or bleeding, the signal intensity on T2-weighted sequences is lower, and fluid-fluid levels can be detected within the cyst due to hemorrhage or detritus (Fig. 16). Hypointense images in the wall of the cyst are occasionally seen in T2-weighted sequences due to dystrophic calcifications associated with infarction. Approximately 50% of ovarian cysts disappear during gestation or after birth [26].

Liver and spleen masses

Prenatal masses in the liver and spleen are rare; they are usually cysts. In the liver, they may appear within the parenchyma or "hang" from the lower edge. They may be single or multiple; multiple cysts usually occur in autosomal recessive polycystic kidney disease. Single cysts usually correspond to a ciliated foregut cyst or epidermoid cyst. Splenic cysts are almost always epidermoid cysts.

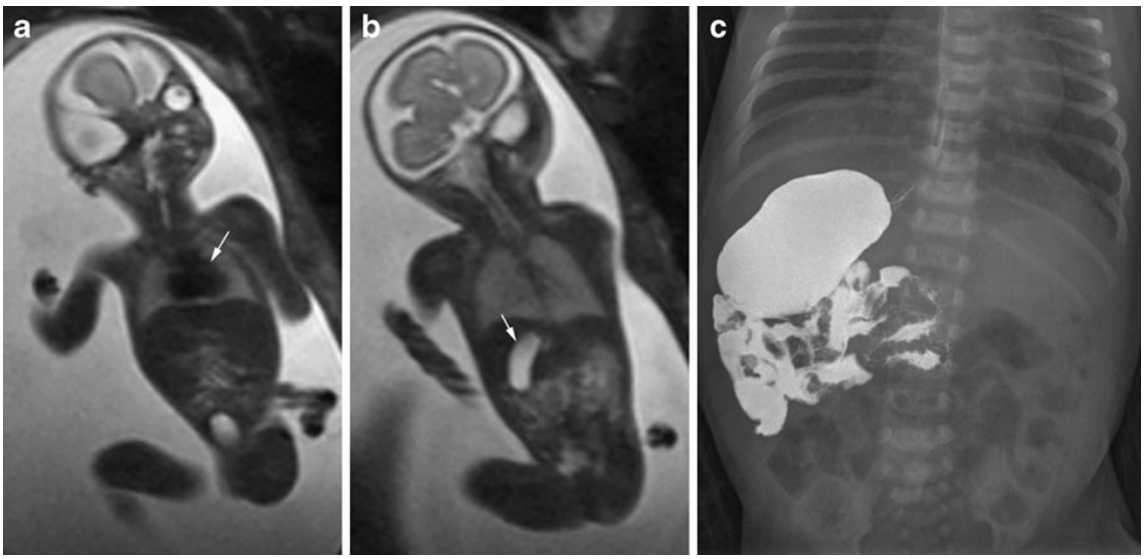

Fig. 14 Heterotaxy syndrome, situs inversus. Fetus at 23 weeks' gestation. **a** and **b** Fetal coronal single-shot fast spin-echo MR images: the heart is in the correct position (*arrow* in **a**) but the stomach is on the right side of the abdomen (*arrow* in **b**). **c** Barium studies after birth confirm this anomaly

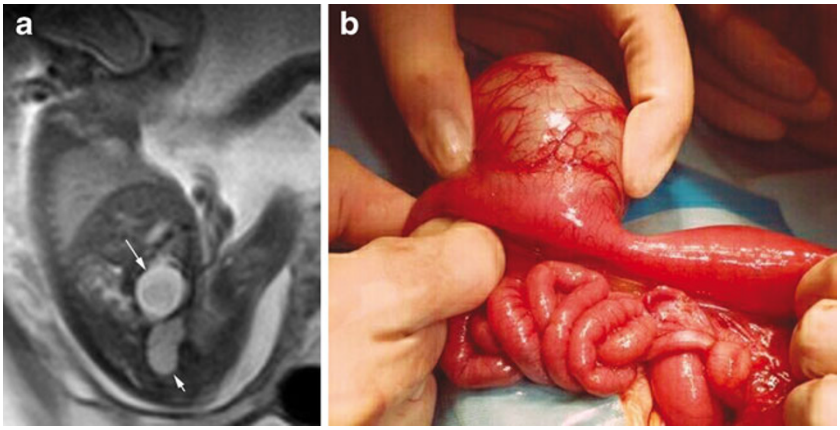

Fig. 15 Intestinal duplication. Fetus at 24 weeks' gestation. **a** Fetal sagittal single-shot fast spin-echo MR image: a hyperintense structure (*long arrow*) is seen above the bladder (*short arrow*); in T1-weighted sequences this lesion was hypointense. The rest of the intestinal loops were normal at MR, but intestinal occlusion with marked dilatation of the intestinal loops was present at birth. Surgical intervention discovered intestinal duplication (**b**). Intestinal duplication caused volvulus of the small intestine

MRI shows rounded structures within the liver or spleen that are hyperintense on T2-weighted sequences, unless they contain blood, in which case fluid-fluid levels can be detected in their interior (Fig. 17).

Other abdominal masses

Neuroblastoma and teratoma are the most common solid neoplasms in infants. More than 90% of prenatally diagnosed neuroblastomas are adrenal in origin, although they may also be located in the thorax or cervical region. About half of these tumors are cystic or heterogeneous [27]. With MRI, solid (Fig. 18), cystic, or more complex lesions can be seen [28] below the diaphragm. Unlike extralobar bronchopulmonary sequestration they are normally in the right side and are almost always detected in the third trimester [10]. These tumors can disappear before birth though they can also metastasize, especially to the fetal liver [27].

Another neonatal tumor is sacrococcygeal teratoma, which appears as cystic, solid, or mixed masses that arise from the sacrococcygeal region. Sacrococcygeal tumors can be completely external, have external and intrapelvic components, or reside predominantly within the pelvis. MRI can

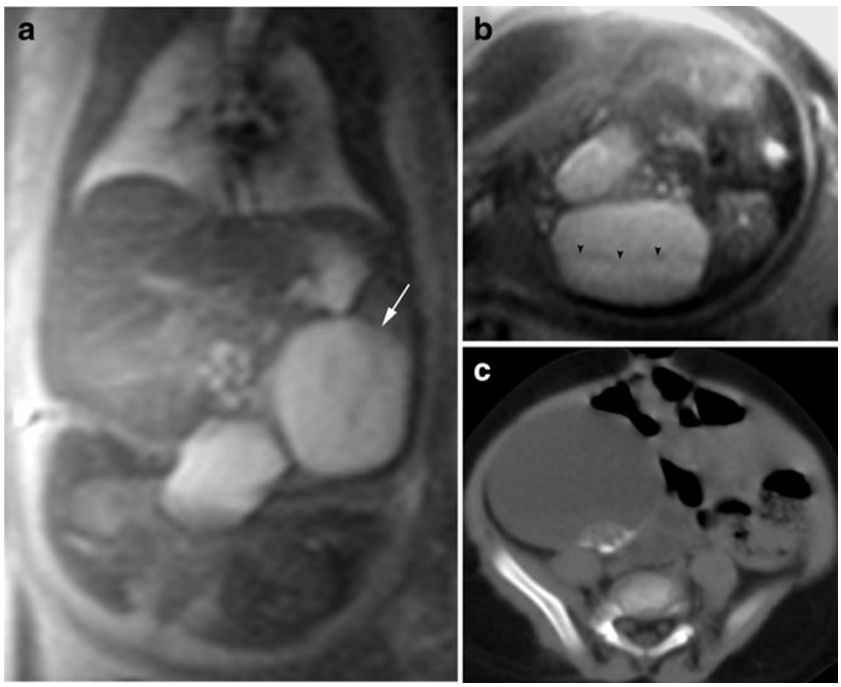

Fig. 16 Ovarian cyst. Fetus at 36 weeks' gestation. **a** Fetal coronal and **b** axial single-shot fast spin-echo MR images showing a rounded hyperintense structure (*arrow*) occupying a large part of the left hemiabdomen, with fluid-fluid level in its interior (*arrowheads* in **b**). **c** CT at 4 months of age: the lesion is now located on the right side and shows calcification of the wall (*arrow*). US follow-up shows complete disappearance of the cyst and also of the right ovary

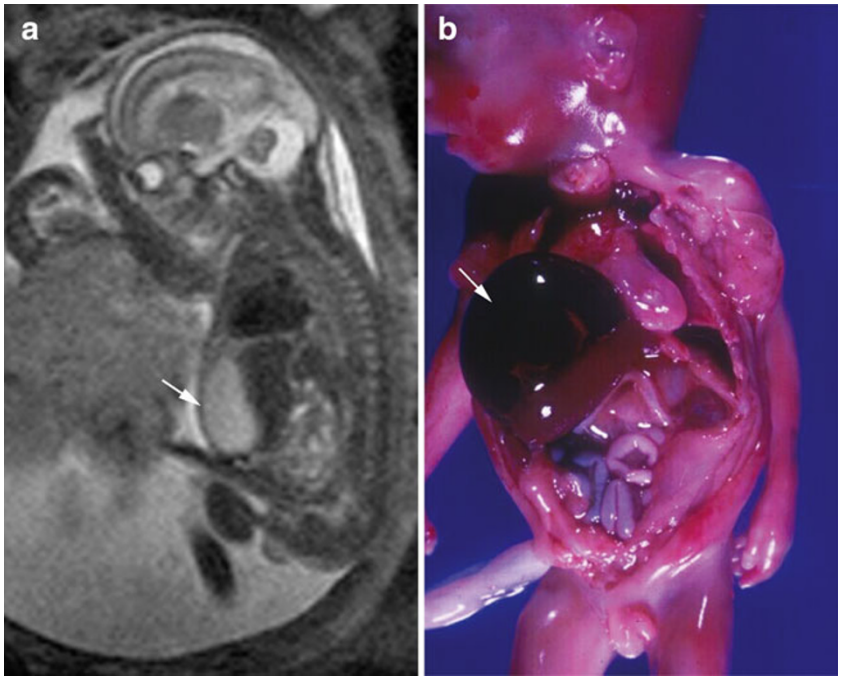

Fig. 17 Hepatic cyst. Fetus at 17 weeks' gestation. **a** Fetal sagittal single-shot fast spin-echo MR image showing a cystic lesion of the liver (*arrow*). This fetus also had agenesis of the right kidney, dysplasia of the left kidney, and heart defects. **b** The hepatic cyst (*arrow*) can be seen in the pathological specimen

help in detecting these lesions and in differentiating them from other solid or cystic masses in the pelvis.

Ventral wall malformations

Gastroschisis

Gastroschisis consists of the herniation of fetal abdominal viscera into the amniotic cavity secondary to a small defect in the abdominal wall involving all the layers of the abdominal wall. It nearly always affects the right side, and the umbilical cord is inserted in its normal position.

MRI easily detects the evisceration of abdominal structures [29, 30]. T2-weighted sequences are the most useful because the abdominal structures located outside the abdominal cavity are clearly visualized against the hyperintense amniotic fluid (Fig. 19). The axial plane is best to show the defect in the abdominal wall and the position of the umbilical cord. T1-weighted sequences are useful for determining the position of the large intestine. Volumetric images can be helpful in determining whether the eviscerated organs

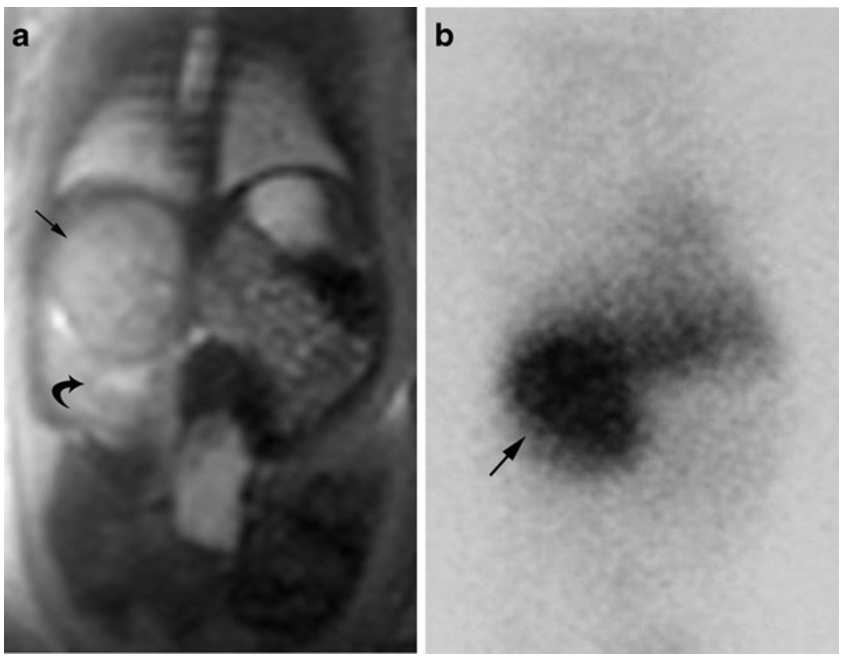

Fig. 18 Neuroblastoma. Fetus at 36 weeks' gestation. **a** Fetal coronal single-shot fast spin-echo MR image showing a well-delimited, slightly heterogeneous infradiaphragmatic mass of intermediate signal intensity (*arrow*) located above the right kidney, which is displaced downward (curved arrow). **b** Metaiodobenzylguandine study after birth was positive (*arrow*)

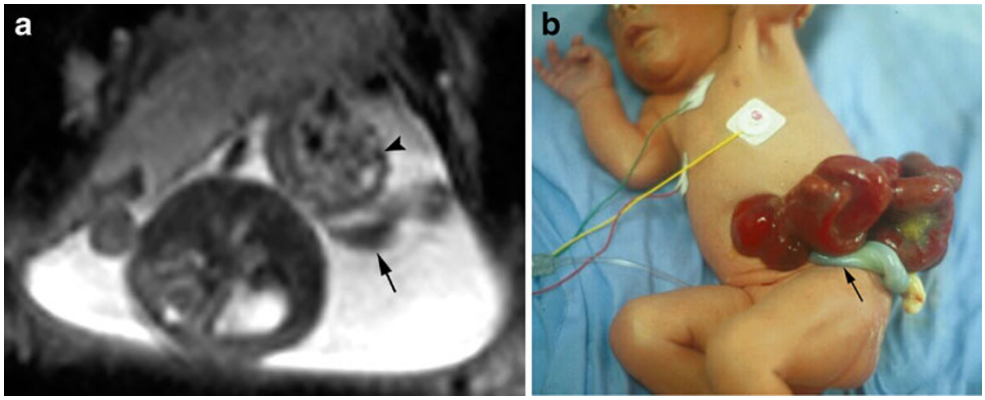

Fig. 19 Gastroschisis. Fetus at 19 weeks' gestation. **a** Fetal axial single-shot fast spin-echo MR image showing a large portion of the intestinal loops outside the abdominal cavity (*arrowhead*). There is no peritoneal lining, and the umbilical cord is inserted in the correct position (*arrow*). The liver and the stomach are within the abdomen. **b** Photograph of the patient after birth showing the intestinal loops outside of the abdominal cavity and the umbilical cord (*arrow*) inserted in the correct position

have a peritoneal lining and the site of umbilical cord insertion. These two findings are important in differentiating gastroschisis from omphalocele (Fig. 20).

Associated anomalies are rare, although intestinal anomalies or complications are common, especially intestinal stenosis or atresia, possibly due to the direct effect of amniotic fluid on the intestinal loops or ischemic problems secondary to compromise of the mesenteric vessels due to the relatively small size of the abdominal wall defect [31].

Fig. 20 Omphalocele. Fetus at 21 weeks' gestation. **a** Fetal axial single-shot fast spin-echo MR image shows the bowel loops lined with peritoneal membranes (*arrow*) outside the abdominal cavity. **b** Volumetric T2 images are useful to identify the umbilical cord (*arrow*). **c** Photograph of the patient after birth showing the intestinal loops outside of the abdominal cavity, the peritoneal membranes, and the position of the umbilical cord (*arrow*)

Omphalocele

In omphalocele, embryologic development is detained at a point in which the developing intestines are located outside of the abdominal cavity. The viscera protrude through a central abdominal wall defect. The herniated viscera are lined with a membrane consisting of two layers: the peritoneum and the amnion. The umbilical cord inserts into the apex of the omphalocele rather than at its normal position. Omphalocele varies considerably in size.

MRI usually enables accurate diagnosis of omphalocele, and its contents are easily determined [30]. MRI also usually shows the linings of the omphalocele and the point of umbilical cord insertion clearly. T2-weighted sequences are the most useful for studying omphalocele, although T1-weighted sequences help in detecting the large intestine, and volumetric sequences help in determining the point of insertion of the umbilical cord (Fig. 20b).

Intestinal complications are less common than in gastroschisis, possibly because the abdominal structures are not in contact with the amniotic fluid and because the defect in the abdominal wall is usually large, making compromised mesenteric blood flow less likely. Omphalocele is often associated with other anomalies and sometimes with chromosomopathies, especially trisomies 18 and 13 [32].

Conclusions

Prenatal awareness of an anomaly ensures better management of the pregnant patient, enables medical teams and parents to prepare for the delivery, and is very useful in deciding postnatal treatment.

Thoracic, gastrointestinal tract, and abdominal anomalies are common and varied, and may be found in association with other anomalies and/or chromosomopathies. Accurate prenatal diagnosis is crucial.

US is the first imaging technique in pregnant women, and MRI is a useful adjunct in most fetal anomalies thanks to its exquisite discrimination among tissues, the possibility of acquiring images in any spatial plane, and the practical absence of the influence of maternal characteristics, fetal position, or fetal and maternal movements. However, not all anomalies can be evaluated with MRI. It is important to recognize the limitations of the technique and bear in mind that its role is to complement US. Fetal MRI should aim to detect lesions and/or anomalies not seen at US and to clarify uncertain or mistaken US findings. MRI is most useful when US has detected or suspected anomalies, and more anomalies are detected when MRI and US findings are assessed together. MRI is indicated whenever an anomaly is detected or suspected at US or from the patient's clinical history.

Acknowledgements The authors thank Mr. John Giba for his assistance with manuscript preparation.

References

1. Martin C, Darnell A, Duran C, Bermúdez P, Mellado F, Rigol S (2004) Magnetic resonance imaging of the intrauterine fetal genitourinary tract: normal anatomy and pathology. Abdom Imaging 29:286–302
2. Martin C, Darnell A, Escofet C, Mellado F, Corona M (2004) Fetal magnetic resonance imaging. Ultrasound Rev Obstet Gynecol 4:214–227
3. Saguintaah M, Couture A, Veyrac C, Baud C, Quere MP (2002) MRI of the fetal gastrointestinal tract. Pediatr Radiol 32:395–404
4. Hubbard AM, Crombleholme TM (1998) Anomalies and malformations affecting the fetal/neonatal chest. Semin Roentgenol 33 (2):117–125
5. Balassy C, Kasprian G, Brugger PC, Weber M, Csapo B, Herold C, Prayer D (2010) Assessment of lung development in isolated congenital diaphragmatic hernia using signal intensity ratios on fetal MR imaging. Eur Radiol 20:829–837
6. Deshmukh S, Rubesova E, Barth R (2010) MR assessment of normal fetal lung volumes: a literature review. AJR 194:W212–W217
7. Cannie MM, Jani JC, De Keyzer F, Allegaert K, Dymarkowski S, Deprest J (2009) Evidence and patterns in lung response after fetal tracheal occlusion: clinical controlled study. Radiology 252:526–533
8. Azizkhan RG, Crombleholme TM (2008) Congenital cystic lung disease: contemporary antenatal and postnatal management. Pediatr Surg Int 24:643–657
9. Daltro P, Werner H, Gasparetto TD, Domingues RC, Rodrigues L, Marchiori E, Gasparetto EL (2010) Congenital chest malformations: a multimodality approach with emphasis on fetal MR imaging. Radiographics 30:385–395
10. Curtis MR, Mooney DP, Vaccaro TJ, Williams JC, Cendron M, Shorter NA, Sargent SK (1997) Prenatal ultrasound characterization of the suprarenal mass: distinction between neuroblastoma and subdiaphragmatic extralobar pulmonary sequestration. J Ultrasound Med 16:75–83
11. Huang CC, Ko SF, Chung MY, Shieh CS, Tiao MM, Lui CC, Ng SH (2004) Infradiaphragmatic pulmonary sequestration combined with cystic adenomatoid malformation: unusual postnatal computed tomographic features. Abdom Imaging 29:439–442
12. Depaepe A, Dolk H, Lechat MF (1993) The epidemiology of tracheo-oesophageal fistula and oesophageal atresia in Europe. EUROCAT Working Group. Arch Dis Child 68:743–748
13. Levine D, Barnewolt CE, Mehta TS, Trop I, Estroff J, Wong G (2003) Fetal thoracic abnormalities: MR imaging. Radiology 228:379–388
14. Langer JC, Hussain H, Khan A, Minkes RK, Gray D, Siegel M, Ryan G (2001) Prenatal diagnosis of esophageal atresia using sonography and magnetic resonance imaging. J Pediatr Surg 36:804–807
15. Dalla Vecchia LK, Grosfeld JL, West KW, Rescorla FJ, Scherer LR, Engum SA (1998) Intestinal atresia and stenosis: a 25-year experience with 277 cases. Arch Surg 133:490–497
16. Haeusler MC, Berghold A, Stoll C, Barisic I, Clementi M, EUROSCAN Study Group (2002) Prenatal ultrasonographic detection of gastrointestinal obstruction: results from 18 European congenital anomaly registries. Prenat Diagn 22:616–623
17. Bailey PV, Tracy TF Jr, Connors RH, Mooney DP, Lewis JE, Weber TR (1993) Congenital duodenal obstruction: a 32-year review. J Pediatr Surg 28:92–95

18. Werler MM, Sheehan JE, Mitchell AA (2003) Association of vasoconstrictive exposures with risks of gastroschisis and small intestinal atresia. Epidemiology 14:349–354
19. Sweeney B, Surana R, Puri P (2001) Jejunoileal atresia and associated malformations: correlation with the timing of in utero insult. J Pediatr Surg 36:774–776
20. Roberts HE, Cragan JD, Cono J, Khoury MJ, Weatherly MR, Moore CA (1998) Increased frequency of cystic fibrosis among infants with jejunoileal atresia. Am J Med Genet 78:446–449
21. Casaccia G, Trucchi A, Nahom A, Aite L, Lucidi V, Giorlandino C, Bagolan P (2003) The impact of cystic fibrosis on neonatal intestinal obstruction: the need for prenatal/neonatal screening. Pediatr Surg Int 19:75–78
22. Veyrac C, Couture A, Saguintaah M, Baud C (2004) MRI of fetal GI tract abnormalities. Abdom Imaging 29:411–420
23. Calvo-Garcia MA, Kline-Fath BM, Levitt MA, Lim FY, Linam LE, Patel MN, Kraus S, Cromblehome TM, Peña A (2011) Fetal MRI clues to diagnose cloacal malformations. Pediatr Radiol 41:1117–1128
24. Applegate KE, Goske MJ, Pierce G, Murphy D (1999) Situs revisited: imaging of the heterotaxy syndrome. Radiographics 19:837–852
25. Levine D, Barnes P, Edelman RR (1999) Obstertric MR imaging. Radiology 211:609–617
26. Heling KS, Chaoui R, Kirchmair F, Stadie S, Bollmann R (2002) Fetal ovarian cysts: prenatal diagnosis, management and postnatal outcome. Ultrasound Obstet Gynecol 20:47–50
27. Acharya S, Jayabose S, Kogan SJ, Tugal O, Beneck D, Leslie D, Slim M (1997) Prenatally diagnosed neuroblastoma. Cancer 80:304–310
28. Hamada Y, Ikebukuro K, Sato M, Tanano A, Kato Y, TakadaK HK (1999) Prenatally diagnosed cystic neuroblastoma. Pediatr Surg Int 15:71–74
29. Shinmoto H, Kashima K, Yuasa Y, Tanimoto A, Morikawa Y, Ishimoto H, Yoshimura Y, Hiramatsu K (2000) MR imaging of non-CNS fetal abnormalities: a pictorial essay. Radiographics 20:1227–1243
30. Shinmoto H, Kuribayashi S (2003) MRI of the fetal abdominal abnormalities. Abdom Imaging 28:877–886
31. Saxena AK, Hülskamp G, Schleef J, Schaarschmidt K, Harms E, Willital GH (2002) Gastroschisis: a 15-year, single-center experience. Pediatr Surg Int 18:420–424
32. Rankin J, Dillon E, Wright C (1999) Congenital anterior abdominal wall defects in the north of England, 1986-1996: occurrence and outcome. Prenat Diagn 19:662–668